EFFECT OF THERMOPHORESIS ON TRANSIENT FREE CONVECTION BOUNDARY LAYER FLOW OF A WALTERS-B FLUID

B. Vasu[1], Rama Subba Reddy Gorla[2], V. R. Prasad[3]

[1]*Department of Mathematics, Motilal Nehru National Institute of Technology Allahabad, (India)*

[2]*Department of Mechanical Engineering, Cleveland State University, Ohio, USA*

[3]*Department of Mathematics, Madanapalle Institute of Technology and Science, (India)*

ABSTRACT

The present paper considers the free convective, unsteady, laminar convective heat and mass transfer in a viscoelastic fluid along an impulsively started vertical plate in presence of thermophoresis. The Walters-B viscoelastic liquid model is employed to simulate medical creams and other rheological liquids encountered in biotechnology and chemical engineering. This rheological model introduces supplementary terms into the momentum conservation equation. The dimensionless unsteady, coupled, and non-linear partial differential conservation equations for the boundary layer regime are solved by an efficient, accurate and unconditionally stable finite difference scheme of the Crank-Nicolson type. The velocity, temperature, and concentration fields have been studied for the effect of thermophoresis, Prandtl number, viscoelasticity parameter, Schmidt number, and buoyancy ratio parameter. The local skin-friction, Nusselt number and Sherwood number are also presented and analyzed graphically. It is observed that, when the viscoelasticity parameter increases, the velocity increases close to the plate surface. An increase in Schmidt number is observed to significantly decrease both velocity and concentration.

Keywords: Unsteady Viscoelastic Flow, Impulsively Vertical Plate, Walters-B Short-Memory Mode, Finite Difference Method, Mass Transfer, Thermophoresis, Schmidt Number.

I. INTRODUCTION

The flow past an impulsively started plate is very important in industrial systems. Such flows are transient and therefore temporal velocity and temperature gradients have to be included in the analysis. The flow of a viscous incompressible fluid past an impulsively started infinite vertical plate, moving in its own plane was first studied by Stokes [1]. Soundalgekar [2] presented an exact solution to the flow of a viscous fluid past an impulsively started infinite isothermal vertical plate. The solution was derived by the Laplace transform technique and the effect of heating or cooling of the plate on the flow field was discussed through Grashof number. Raptis and Singh [3] studied the flow past an impulsively started infinite vertical plate in a Porous medium by a finite difference method. Muthucumaraswamy and Ganesan [4] studied the unsteady flow past an impulsively started isothermal vertical plate with mass transfer by an implicit finite difference method. Viscoelastic flows arise in numerous processes in chemical engineering systems. Such flows possess both viscous and elastic properties and can exhibit normal stresses and relaxation effects. An extensive range of mathematical models has been developed to simulate the diverse hydrodynamic behaviour of these non-Newtonian fluids. An eloquent exposition of viscoelastic fluid models has been presented by Joseph [5]. Examples of such models are the Rivlin-Ericksen second order model, the Oldrotd model, Johnson-Segalman model, the upper convected Maxwell model and the Walters-B model [6]. Both steady and unsteady flows have been investigated at length in a diverse range of geometries using a wide spectrum of analytical and computation methods. The Walters-B viscoelastic model [6] was developed to simulate viscous fluids possessing short memory elastic effects and can simulate accurately many complex polymeric, biotechnological and tri-biological fluids. The Walters-B model has therefore been studied extensively in many flow problems. Soundalegkar and Puri [7] presented one of the first mathematical investigations for such a fluid considering the oscillatory two-dimensional viscoelastic flow along an infinite porous wall, showing that an increase in the Walters elasticity parameter and the frequency parameter reduces the phase of the skin-friction. Chang et al [8] analyzed the unsteady buoyancy-driven flow and species diffusion in a Walters-B viscoelastic flow along a vertical plate with transpiration effects. Nanousis [9] used a Laplace transform method to study the transient rotating hydromagnetic Walters-B viscoelastic flow regime. Thermophoresis is a radiometric force by temperature gradient that enhances small particles moving toward a cold surface and away from a hot one. It plays a significant role on particle transport in laminar boundary layer flow. Generally, the mainly effect of thermophoresis on small particle size is especially effective in a range of *dp* = 0.01-1.0 μ*m*. Thermophoresis on particle deposition onto a surface in laminar boundary layer flow is now rather well understood theoretically. Goren [10] developed the thermophoretic deposition of particles in a laminar compressible boundary layer flow past a flat plate. There are some other proposed models for particle deposition by coupled of thermophoresis and Brownian diffusion (Batchelor and Shen [11]). Chamkha *et al*. [12] studied the effect of thermophoretic force in free convection boundary layer from a vertical flat plate embedded in a porous medium with heat generation or absorption. Partha [13] used similarity technique to obtain the solutions about effect of suction/injection on thermophoretic particle deposition in free convection onto a vertical plate embedded in a fluid saturated non-Darcy porous medium. In recent years, non-Newtonian fluids have been appearing in increasing numbers. In spite of the extensive research over the past few decades which dealt with the flow of non-Newtonian fluids, there has been little work done on the unsteady flow for non-Newtonian fluids. To our best knowledge, study on thermophoresis effects on Walters-B viscoelastic fluid flow past an impulsively started vertical plate has never been considered before. Therefore, in this paper we investigate the effects of thermophoretic parameter in the Walters-B model over the vertical plate. The transformed boundary layer equations are solved with a versatile, validated implicit finite difference procedure, benchmarked where appropriate with previous studies. The values of skin friction, wall heat transfer and wall deposition flux are also tabulated. Another motivation of the study is to further investigate the observed high heat transfer performance commonly attributed to extensional stresses in viscoelastic boundary layers.

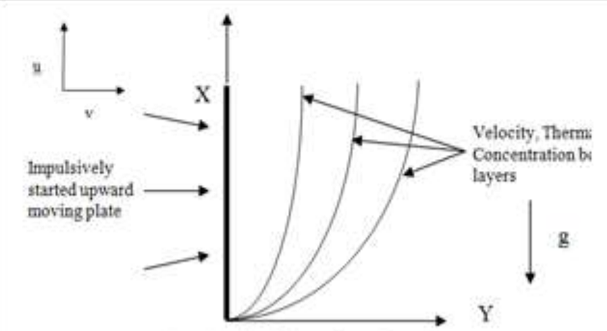

Fig 1(a) Physical model and coordinate system

II. MATHEMATICAL FORMULATION

An unsteady two-dimensional laminar free convective flow of a viscoelastic fluid past an impulsively started vertical plate is considered. The x-axis is taken along the plate in the upward direction and the y-axis is taken normal to it. The physical model is shown in Fig.1. Initially, it is assumed that the plate and the fluid are at the same temperature T'_∞ and concentration level C'_∞ everywhere in the fluid. At time, t'>0, the plate starts moving impulsively in the vertical direction with constant velocity u_0 against the gravitational field. Also, the temperature of the plate and the concentration level near the plate are raised to T'_w and C'_w respectively and are maintained constantly thereafter. It is assumed that the concentration C' of the diffusing species in the binary mixture is very less in comparison to the other chemical species, which are present, and hence the Soret and Dufour effects are negligible. It is also assumed that there is no chemical reaction between the diffusing species and the fluid. Then, under the above assumptions, the governing boundary layer equations with Boussinesq approximation are

$$\frac{\partial u}{\partial x}+\frac{\partial v}{\partial y}=0 \tag{1}$$

$$\frac{\partial u}{\partial t'}+u\frac{\partial u}{\partial x}+v\frac{\partial u}{\partial y}=g\beta\left(T'-T'_\infty\right)+g\beta^*\left(C'-C'_\infty\right)+\nu\frac{\partial^2 u}{\partial y^2}-k_0\frac{\partial^3 u}{\partial y^2\partial t'} \tag{2}$$

$$\frac{\partial T'}{\partial t'}+u\frac{\partial T'}{\partial x}+v\frac{\partial T'}{\partial y}=\frac{k}{\rho c_p}\frac{\partial^2 T'}{\partial y^2} \tag{3}$$

$$\frac{\partial C'}{\partial t'}+u\frac{\partial C'}{\partial x}+v\frac{\partial C'}{\partial y}=D\frac{\partial^2 C'}{\partial y^2}-\frac{\partial}{\partial y}\left(c'v_t\right) \tag{4}$$

The initial and boundary conditions are

$$\begin{aligned}
&t'\le 0: u=0, v=0, T'=T'_\infty, C'=C'_\infty \\
&t'>0: u=u_0, v=0, T'=T'_w, C'=C'_w \qquad at\ y=0 \\
&\qquad u=0, T'=T'_\infty, C'=C'_\infty \qquad at\ x=0 \\
&\qquad u\to 0, T'\to T'_\infty, C'\to C'_\infty \qquad as\ y\to\infty
\end{aligned} \tag{5}$$

Where u, v are velocity components in x, y directions respectively, t' - the time, g - the acceleration due to gravity, β - the volumetric coefficient of thermal expansion, β^* - the volumetric coefficient of expansion with concentration, T' -the temperature of the fluid in the boundary layer, C' -the species concentration in the boundary layer, T'_w - the wall temperature, T'_∞ - the free stream temperature far away from the plate, C'_w - the concentration at the plate, C'_∞ - the free stream concentration in fluid far away from the plate, ν - the kinematic viscosity, α - the thermal diffusivity, ρ - the density of the fluid and D - the species diffusion coefficient.

On introducing the following non-dimensional quantities

$$X=\frac{xu_0}{\nu},Y=\frac{yu_0}{\nu},U=\frac{u}{u_0},V=\frac{v}{u_0},t=\frac{t'u_0{}^2}{\nu},Sc=\frac{\nu}{D},T=\frac{T'-T'_\infty}{T'_w-T'_\infty},C=\frac{C'-C'_\infty}{C'_w-C'_\infty},$$
$$\Gamma=\frac{k_0u_0{}^2}{\nu^2},\Pr=\frac{\nu}{\alpha},\tau=\frac{k\nu(T'_w-T'_\infty)}{T_wu_0},Gr=\frac{\nu g\beta(T'_w-T'_\infty)}{u_0{}^3},Gm=\frac{\nu g\beta^*(C'_w-C'_\infty)}{u_0{}^3} \tag{6}$$

Equations (1), (2), (3), (4) and (5) are reduced to the following non-dimensional form

$$\frac{\partial U}{\partial X}+\frac{\partial U}{\partial Y}=0 \tag{7}$$

$$\frac{\partial U}{\partial t}+U\frac{\partial U}{\partial X}+V\frac{\partial U}{\partial Y}=\frac{\partial^2 U}{\partial Y^2}+GrT+GmC-\Gamma\frac{\partial^3 U}{\partial Y^2\partial t} \tag{8}$$

$$\frac{\partial T}{\partial t}+U\frac{\partial T}{\partial X}+V\frac{\partial T}{\partial Y}=\frac{1}{\Pr}\frac{\partial^2 T}{\partial Y^2} \tag{9}$$

$$\frac{\partial C}{\partial t}+U\frac{\partial C}{\partial X}+V\frac{\partial C}{\partial Y}=\frac{1}{Sc}\frac{\partial^2 C}{\partial Y^2}+\frac{\tau}{Gr^{1/4}}\left[\frac{\partial C}{\partial Y}\frac{\partial T}{\partial Y}+C\frac{\partial^2 T}{\partial Y^2}\right] \tag{10}$$

The corresponding initial and boundary conditions are

$$\begin{aligned}
&t\le 0: U=0,\ V=0,\ T=0,\ C=0\\
&t>0:\ U=1,\ V=0,\ T=1,\ C=1 \qquad at \qquad Y=0\\
&\qquad U=0,\ T=0,\ C=0 \qquad at \qquad X=0\\
&\qquad U\to 0,\ T\to 0,\ C\to 0 \qquad as \qquad Y\to\infty
\end{aligned} \tag{11}$$

where *Gr* is the thermal Grashof number, *Pr* is the fluid Prandtl number, *Sc* is the Schmidt number, *Gm* is the solutal Grashof number and Γ is the viscoelastic parameter.

To obtain an estimate of flow dynamics at the barrier boundary, we also define several important rate functions at Y = 0. These are the dimensionless wall shear stress function, i.e. local skin friction function, the local Nusselt number (dimensionless temperature gradient) and the local Sherwood number (dimensionless species, i.e. contaminant transfer gradient) are computed with the following mathematical expressions

$$\tau_X=-\left(\frac{\partial U}{\partial Y}\right)_{Y=0},\quad Nu_x=-X\left(\frac{\partial T}{\partial Y}\right)_{Y=0},\quad Sh_X=-X\left(\frac{\partial C}{\partial Y}\right)_{Y=0} \tag{12}$$

We note that the dimensionless model defined by Eqns. (7) to (10) under conditions (11) reduces to Newtonian flow in the case of vanishing viscoelasticity i.e. when $\Gamma\to 0$.

III. NUMERICAL SOLUTION

In order to solve these unsteady, non-linear coupled equations (7) to (10) under the conditions (11), an implicit finite difference scheme of Crank-Nicolson type has been employed. This method was originally developed for heat conduction problems [14]. Prasad et al [15] described the solution procedure in detail. The region of integration is considered as a rectangle with $X_{\max}=1$ and $Y_{\max}=14$ where $Y_{\max}$ corresponds to $Y=\infty$ which lies well outside the momentum, thermal and concentration boundary layers. After some preliminary numerical experiments the mesh sizes have been fixed as $\Delta X=0.05$, $\Delta Y=0.25$ with time step $\Delta t=0.01$.

The computations are executed initially by reducing the spatial mesh sizes by 50% in one direction, and later in both directions by 50% and the results are compared. It is observed that, in all the cases, the results differ only in the fifth decimal place. Hence these mesh sizes are considered to be appropriate mesh sizes for present calculations. The local truncation error in the finite difference approximation is $O(\Delta t^2 + \Delta X + \Delta Y^2)$ and it tends to zero as $\Delta t, \Delta X$ and ΔY tend to zero. Hence the scheme is compatible. The scheme is unconditionally stable and explained in detail by Prasad et al. [15] and Vasu and Manish [16]. Stability and compatibility ensures convergence.

IV. RESULTS AND DISCUSSION

A representative set of numerical results is presented graphically to illustrate the influence of viscoelastic parameter *Γ*, thermophoretic parameter *τ*, Grashof number *Gr*, mass Grashof number *Gm*, Schmidt number *Sc* on the velocity, temperature, concentration, skin-friction, Nusselt number and Sherwood number. *Pr* defines the

Gr=Gm	τ	X = 0.1			X = 0.5			X = 1.0		
		τ_x	Nux	Shx	τ_x	Nux	Shx	τ_x	Nux	Shx
0.0	0.0	3.48356	0.14283	0.15065	1.00545	0.23450	0.38949	0.67170	0.32328	0.70751
	0.1	3.48356	0.14283	0.14072	1.00545	0.23450	0.36609	0.67170	0.32328	0.67117
	0.5	3.48356	0.14283	0.09884	1.00545	0.23450	0.26522	0.67170	0.32328	0.51290
	1.0	3.48356	0.14283	0.04034	1.00545	0.23450	0.11602	0.67170	0.32328	0.27231
0.2	0.0	3.34829	0.14977	0.15519	0.68704	0.27542	0.41870	0.24776	0.40430	0.77784
	0.1	3.34688	0.14988	0.14510	0.68436	0.27592	0.39375	0.24432	0.40519	0.73827
	0.5	3.34066	0.15039	0.10260	0.67222	0.27821	0.28654	0.22865	0.40937	0.56740
	1.0	3.33136	0.15119	0.04346	0.65289	0.28201	0.12997	0.20306	0.41645	0.31446
1.0	0.0	2.86312	0.16519	0.16661	-0.38096	0.33911	0.47610	-1.11375	0.52132	0.90380
	0.1	2.85724	0.16546	0.15610	-0.39091	0.34003	0.44918	-1.12577	0.52284	0.86061
	0.5	2.83186	0.16666	0.11194	-0.43499	0.34417	0.33470	-1.17938	0.52975	0.67665
	1.0	2.79503	0.16845	0.05089	-0.50223	0.35062	0.17178	-1.26238	0.54071	0.41367
5.0	0.0	0.83466	0.20210	0.19678	-4.59606	0.45555	0.59469	-6.28649	0.72420	1015131
	0.1	0.81089	0.20265	0.18516	-4.63054	0.45698	0.56440	-6.32538	0.72644	1.10277
	0.5	0.70942	0.20502	0.13637	-4.77976	0.46322	0.43756	-6.49448	0.73635	0.89961
	1.0	0.56547	0.20841	0.06906	-4.99703	0.47245	0.26328	-6.74311	0.75124	0.62047

ratio of momentum diffusivity (ν) to thermal diffusivity. The values of *Sc* are chosen such that they represent water vapor (0.6), Ammonia (0.78), Carbon dioxide (0.94) and Ethyl Benzene (2.0). Selected computations are presented in Figures and tables. The default values for the control parameters are selected as: *Γ* = 0.005, τ = 0.5, *Sc* = 0.6, *Pr* = 0.71 (air) and *Gr* = *Gm* = 2, 4.

In Tables 1 the variation of dimensionless local skin friction τ_X Nusselt number Nu_X and the Sherwood number Sh_X , for various *Gr* or *Gm* and thermophoretic parameters (τ) at different *X* = 0.1, 0.5 and 1.0 along the plate are tabulated in Table 1(a). Shear stress is clearly decreased with increasing the values of *Gr* or *Gm*, whereas Nu_X and Sh_X increases with an increase in the values of *Gr* or *Gm*. The opposite behaviour is observed for increasing thermophoretic parameter τ

Gr = Gm	Γ	X = 0.1			X = 0.5			X = 1.0		
		τx	Nux	Shx	τx	Nux	Shx	τx	Nux	Shx
0.0	0.000	2.33434	0.17850	0.11768	0.70438	0.27825	0.27405	0.47338	0.37546	0.52798
	0.003	2.86552	0.16138	0.10821	0.84489	0.25660	0.26997	0.56658	0.34879	0.52201
	0.005	3.48356	0.14283	0.09884	1.00545	0.23450	0.26522	0.67170	0.32328	0.51290
0.2	0.000	2.25584	0.18089	0.11925	0.51296	0.29935	0.28840	0.21306	0.42504	0.56371
	0.003	2.75818	0.16567	0.11070	0.58956	0.28785	0.28769	0.22322	0.41618	0.56602
	0.005	3.34066	0.15039	0.10260	0.67222	0.27821	0.28654	0.22865	0.40937	0.56740
1.0	0.000	1.95737	0.18861	0.12439	-0.15840	0.34658	0.32472	-0.65434	0.51917	0.64588
	0.003	2.36179	0.17725	0.11785	-0.28198	0.34500	0.32988	-0.89291	0.52445	0.66147
	0.005	2.83186	0.16666	0.11194	-0.43499	0.34417	0.33470	-1.17938	0.52975	0.67665
5.0	0.000	0.64077	0.21334	0.14111	-2.84205	0.44634	0.40943	-3.97098	0.69877	0.82686
	0.003	0.66542	0.20885	0.13853	-3.72700	0.45518	0.42383	-5.12525	0.71868	0.86361
	0.005	0.70942	0.20502	0.13637	-4.77976	0.46322	0.43756	-6.49448	0.73635	0.89961

Table 2 show that the values of local skin friction τ_X Nusselt number Nu_X and the Sherwood number Sh_X for different Gr, Gm and Γ at X = 0.1, 0.5 and 1.0. It is observed that an increase in the values of viscoelastic parameter Γ causes an increase in the shear stress rate at various X = 0.1, 0.5 and 1.0. It is also observed that the reverse behaviour for Nu_X , Sh_X .

Sc	Pr = 0.01			Pr = 0.71			Pr = 7.0		
	τx	Nux	Shx	τx	Nux	Shx	τx	Nux	Shx
0.25	-3.57960	0.09803	0.74851	-2.84827	0.63359	0.56013	-2.26594	1.93322	0.28518
0.60	-3.39355	0.09765	1.04682	-2.67080	0.60660	0.75601	-2.16310	1.91450	0.15704
0.78	-3.33503	0.09756	1.15543	-2.61676	0.59942	0.82357	-2.14869	1.91135	0.07018
0.94	-3.29292	0.09750	1.23871	-2.57835	0.59466	0.87381	-2.14593	1.91029	-0.01245
2.0	-3.12046	0.09731	1.63069	-2.42482	0.57827	1.08969	-2.24432	1.92417	-0.62059
5.0	-2.91296	0.09714	2.22222	-2.25194	0.56411	1.32786	-3.90130	2.19475	-4.50153

From **Table 3** we observed that the variation of τ_X , Nu_X and Sh_X for various *Sc* and Pr at various *X* = 0.1, 0.5 and 1.0 along the plate. The local Nusselt number values decreases with increases in *Sc*, whereas τ_X and Sh_X increases with an increase in the values of *Sc*. The same behaviour is observed for increasing Pr also.

In Figures 2(a) to 2(c), we have presented the variation of the velocity, temperature and concentration with collective effects of thermophoretic parameter (τ) and Schmidt number (Sc) at X = 1.0. Sc defines the ratio of momentum diffusivity (ν) to molecular diffusivity (*D*). For Sc<1, species will diffuse much faster than momentum so that maximum concentrations will be associated with this case (Sc = 0.6). For Sc > 1, momentum will diffuse faster than species causing progressively lower concentration values. With an increase in molecular diffusivity concentration boundary layer thickness is therefore increased. For the special case of *Sc* = 1, the species diffuses at the same rate as momentum in the viscoelastic fluid. Both concentration and boundary layer thicknesses are the same for this case. An increase in Schmidt number

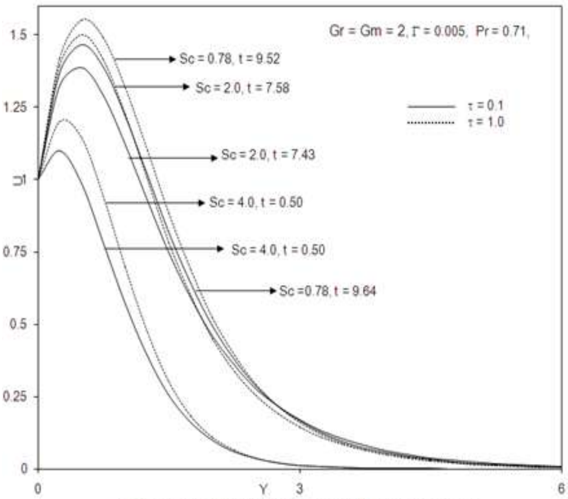

Fig 2(a). Steady state velocity profiles at X=1 for different Sc and τ

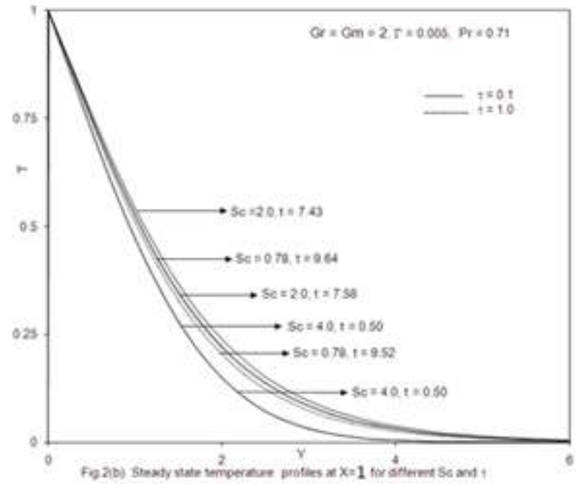

Fig 2(b) Steady state temperature profiles at X=1 for different Sc and τ

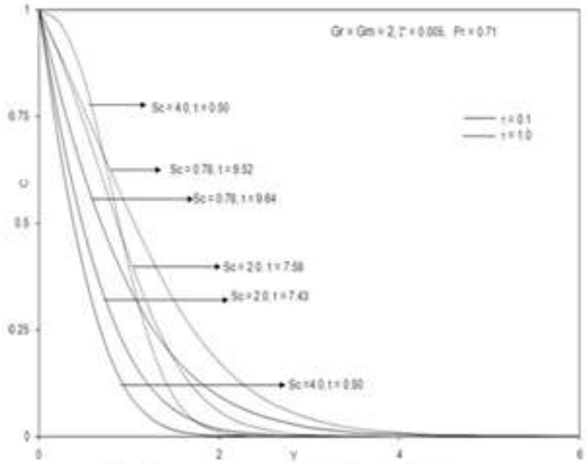

Fig 2(c) Steady state concentration profiles at X=1 for different Sc and τ

effectively depresses concentration values in the boundary layer regime since higher *Sc* values will physically manifest in a decrease of molecular diffusivity (*D*) of the viscoelastic fluid i.e. a reduction in the rate of mass diffusion. Lower *Sc* values will exert the reverse influence since they correspond to higher molecular diffusivities. Concentration boundary layer thickness is therefore considerably greater for $Sc = 0.6$ than for $Sc = 2.0$. From Figure 2(a), it is seen that an increase in the values of τ from 0.0 to 1.0 leads to enhance the velocity for different values of *Gr*, *Gm*, *Sc*, Γ and for fluid Prandtl number *Pr* (=0.71). It is also observed that the velocity decreases due to increase in *Sc*. Figure 2(b) shows that the temperature decreases throughout the boundary layer with the increasing values of τ. all profiles decay from the maximum at the wall to zero in the free stream. The graphs show therefore that increasing thermophoretic parameter cools the flow. It is also observed that the temperature profiles decreases due to an increase in the values of Sc. From Figure 2(c), it is noticed that an increase in the values of τ from 0.0 to 1.0 leads to an increase in the concentration. It is also observed that the concentration decreases due to increase in the values of Schmidt number. Concentration values are also seen to increase continuously with time t. An increase in Schmidt number effectively depresses concentration values in the boundary layer regime since higher Sc values will physically manifest in a decrease of molecular diffusivity (D) of the viscoelastic fluid i. e. a reduction in the rate of mass diffusion. Lower Sc values will exert the reverse influence since they correspond to higher molecular diffusivities.

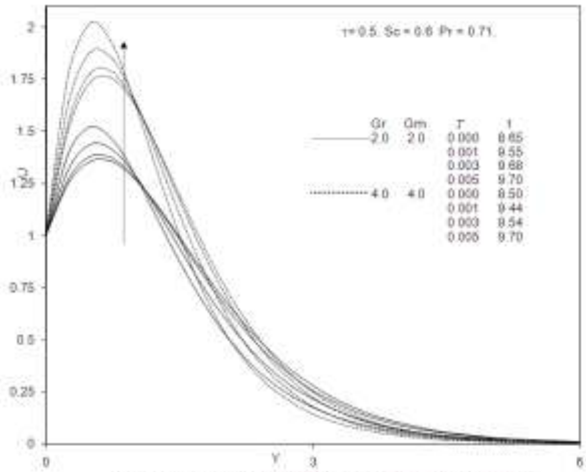

Fig 3(a) Steady state velocity profiles at X= 1 for different Gr, Gm and Γ

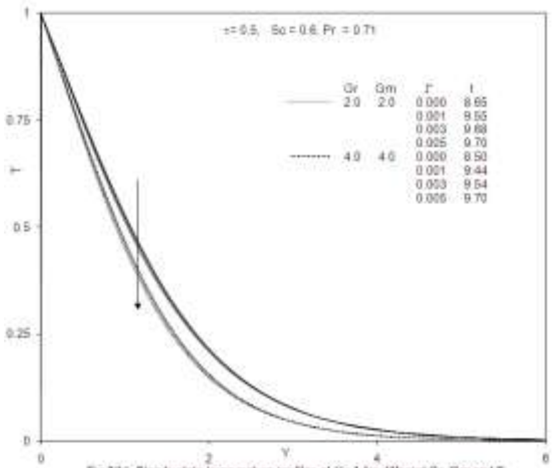

Fig 3(b) Steady state temperature profiles at X= 1 for different Gr, Gm and Γ

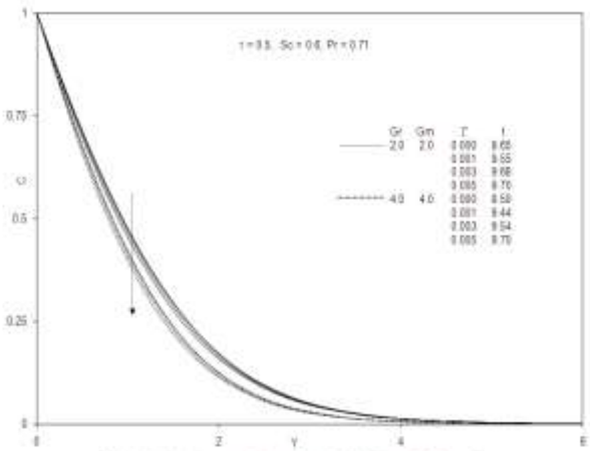

Fig3(c) Steady state concentration profiles at X=1 for different Gr, Gm and Γ

Figures 3(a) to 3(c) illustrate the effect of viscoelastic parameter (Γ), Grashof number *Gr*, mass Grashof number *Gm* on the velocity, temperature and concentration at X=1.0. From Figure 3(a), it is observed that the velocity increases due to an increase in the values of *Gr* or *Gm*. With increasing the values of Γ from 0.000 through 0.001, 0.003 to the maximum value of 0.005, clearly enhances the velocity which ascends sharply and peaks in close vicinity to the plate (Y=0). With increasing distance from the plate however the velocity is adversely affected by increasing the values of Γ, i.e. the flow is decelerated. Therefore close to the plate the flow velocity is maximized for the case of $\Gamma = 0$. But this trend is reversed as we progress further into the boundary layer regime. The switchover in behavior corresponds to approximately Y =1.5, with increasing velocity profiles decay smoothly to zero in the free stream at the edge of the boundary layer. The opposite effect is caused by an increase in time. A rise in t from 8.65, through 9.55, 9.68 and to the maximum value of 9.70 causes an increase in flow velocity near the wall, in this case the maximum velocity arises for the largest time progressed. Again there is a reverse in the response at Y =1.5, and thereafter velocity is maximized with the least value of time. From Figure 3(b), it is observed that the temperature decreases with an increase in the values of *Gr* or *Gm*. With increasing the values of Γ causes a decrease in the temperature decreases both in the near-wall regime and the far-field regime of the boundary layer. As we approach the free stream the effects of viscoelastic parameter Γ are negligible since the profiles are all merged together. From Figure 3(c), it is observed that an increase in the values of *Gr* or *Gm* causes a decrease in the concentration. It is also observed that the concentration decreases throughout the boundary layer due to an increase in Γ. All profiles decay from the maximum at the wall to zero in the free stream.

V. CONCLUSIONS

A two-dimensional, unsteady laminar incompressible boundary layer model has been presented for the external flow, heat and mass transfer in a viscoelastic buoyancy-driven flow past an impulsively started vertical plate under the influence of thermophoresis. The Walters-B viscoelastic model has been employed which is valid for short memory polymeric fluids. The dimensionless conservation equations have been solved with the well-tested, robust, highly efficient, implicit Crank-Nicolson finite difference numerical method.

The present computations have shown that

- Increasing thermophoretic parameter accelerates the velocity and concentration, but reduces the temperature.
- Increasing viscoelastic parameter accelerates the velocity, but reduces the temperature and concentration.
- Increasing Gr or Gm accelerates the velocity, but reduces the temperature and concentration.
- Increasing Schmidt number accelerates the temperature, but reduces the velocity and concentration.

- Increasing thermophoretic parameter decreases the dimensionless wall shear stress function, i.e. local skin friction function and mass transfer rate (local Sherwood number). At the plate with the opposite effect sustained for the local heat transfer rate (local Nusselt number)

VI. ACKNOWLEDGEMENTS

One of the authors (B Vasu) is thankful to the Motilal Nehru National Institute of Technology Allahabad, India, for the financial support under the Cumulative Professional Development Allowance [CPDA].

REFERENCES

[1] G. G. Stokes., On the effect of internal friction of fluids on the motion of pendulums, *Cambridge Phil. Trans., 9*, 1995, 8-106.

[2] V. M. Soundalgekar., Free convection and mass transfer effects on the viscoelastic flow past an impulsively-started vertical plate, *ASME J. Applied Mechanics*, 46, 1979, 757-760.

[3] A. Raptis and A. K. Singh., free convection flow past an impulsively started vertical plate in a porous medium by finite difference method. *Astro physics and Space Science. 112*, 1985, 259-265.

[4] R. Muthucumaraswamy and P. Ganesan., The first order chemical reaction on flow past an impulsively started vertical plate with uniform heat and mass flux. *Acta. Mech*. *147*, 2001, 45-47.

[5] D.D. Joseph, *Fluid dynamics of viscoelastic liquids* (Springer-Verlag, New York, 1990)

[6] K. Walters., Non-Newtonian effects in some elastico-viscous liquids whose behaviour at small rates of shear is characterized by a general linear equation of state, *Quart. J. Mech. Applied. Math., 15*, 1962, 63-76.

[7] V. M. Soundalgekar and P. Puri On fluctuating flow of an elastico-viscous fluid past an infinite plate with variable suction, *J. Fluid Mechanics, 35(3)*, 1969, 561-573.

[8] T.B. Chang, Bég, O. Anwar, J. Zueco and M. Narahari, Numerical study of transient free convective mass transfer in a Walters-B viscoelastic flow with wall suction, *Comm. in Nonlinear Sci and Num Sim, 16*, 2011, 216-225.

[9] N. Nanousis, Unsteady magnetohydrodynamic flows in a rotating elasto-viscous fluid, *Astrophysics and Space Science, 199(2)*, 1993, 317-321.

[10] S. L. Goren., Thermophoresis of aerosol particles in the laminar boundary layer on a flat surface, *Journal of Colloid and Interface Science, 61*, 1977, 77-85.

[11] G. K. Batchelor, and C. Shen., Thermophoretic deposition in gas flow over cold surfaces, *Journal of Colloid and Interface Science, 107*, 1985, 21-37.

[12] A. J. Chamkha, A. F. Al-Mudhaf and I. Pop., Effect of heat generation or absorption on thermophoretic free convection boundary layer from a vertical flat plate embedded in a porous medium, *International Communications in Heat and Mass Transfer, 33*, 2006, 1096-1102.

[13] M. K. Partha., Suction/injection effects on thermophoresis particle deposition in a non-Darcy porous medium under the influence of Soret, Dufour effects, *International Journal of Heat and Mass Transfer, 52*, 2009, 1971-1979.

[14] J. Crank, and P. Nicolson, A practical method for numerical evaluation of solutions of partial differential equations of the heat conduction type, *Proc. Camb. Phil. Society*, *43*, 1947, 50-67.

[15] V. R. Prasad, N. Bhaskar Reddy and R. Muthucumaraswamy, Radiation and mass transfer effects on two-dimensional flow past an impulsively started infinite vertical plate, *Int. J. Thermal Sciences*, *46(12)*, 2007, 1251-1258.

[16] Vasu B and Manish K, Transient Boundary Layer Laminar Free Convective Flow of a Nanofluid over a Vertical Cone/Plate, International Journal of Applied and Computational Mathematics, January 2015, DOI: 10.1007/s40819-015-0027-9, Article in press.